Validation of the Scatter Fraction Obtained from the Cylindrical Phantom for Calculating Noise Equivalent Count in Clinical PET Examinations

Shota Hosokawa¹⁾, Kazumasa Inoue²⁾*, Yasuyuki Takahashi¹⁾, Daisuke Kano^{3,5)}, Yoshihiro Nakagami^{4,6)}, Shuto Nakazawa²⁾, Katsumasa Suzaki⁷⁾ and Masahiro Fukushi²⁾

Graduate School of Health Sciences, Department of Radiation Science, Hirosaki University
 Graduate School of Human Health Sciences, Department of Radiological Sciences,
 Tokyo Metropolitan University

3)Department of Pharmacy, National Cancer Center Hospital East
4)Department of Diagnostic Radiology, National Cancer Center Hospital East
5)Department of Diagnostic Radiology, Tokyo Medical and Dental University
6)Yokohama City University School of Medicine Medical Course Radiology
7)Department of Medical Technology Division of Radiology, Hirosaki University Hospital

* corresponding author

(article received : Jun 18, 2019)

Key words: PET/CT, Image quality evaluation, Monte Carlo simulation, Scatter fraction, Noise equivalent count

1. Introduction

Therapy evaluation using fluorodeoxyglucose-positron emission tomography/computed tomography (FDG-PET/CT) is widely used, and multi-center clinical trials using this device are increasing yearly ^{1,2)}. Under such circumstances, their image quality must be identical. However, different types of PET devices are used in each hospital. Therefore, the variation in PET image quality, depending on condition of acquisition and image reconstruction, is currently a major problem^{3,4)}. The progress of hardware and software complicates the relationship between the amount of counts and image quality. Radiomics using multiple indicator was useful for the prediction of the PET image quality⁵⁾. We investigated the accuracy of the calculation method of each indicator. The Japanese acquisition guideline^{6,7)} recommends that the clinical image quality should be evaluated using noise equivalent count patient (NEC_{patient}), NEC density

(NEC_{density}), and signal-to-noise ratio in the liver (SNR_{liver}). These evaluation indicators contributed to standardization of the acquisition $protocol^{8\sim10)}$. Originally, we should use SF obtained from each patient to calculate NEC. However, a PET device cannot discriminate scatter from non-scatter because of poor energy discriminant ability. The SF that was determined by each PET device was written in Digital Imaging and Communications in Medicine (DICOM) standard image header. However, the Japanese acquisition guideline^{6,7)} recommended that the method was unreliable because estimation method is unclear. Thus, we substituted the device-fixed scatter fraction (SF_{fix}) that was obtained from cylindrical phantom for true SF even though there are few studies on the use of $SF_{\rm fix}$ for NEC calculations. This study aimed to validate the use of SFfix for NEC calculations through a comparative analysis of SF estimated through Monte Carlo simulations using clinical PET/CT image data (SF_{sim}) and SF written in DICOM header (SF_{hdr}).

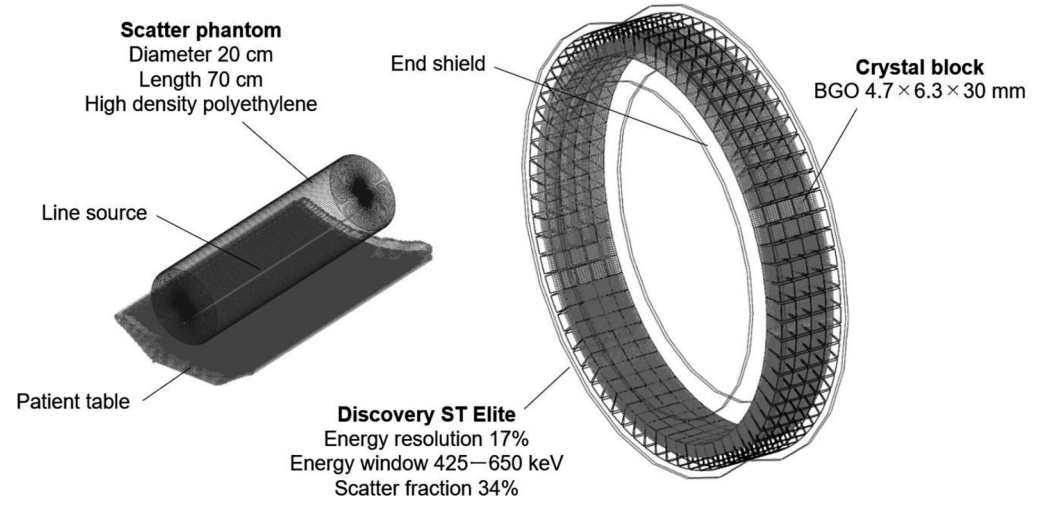


Fig. 1 The appearance of PET device and scatter phantom. We simulated PET device (Discovery ST Elite, GE) and scatter phantom by using Monte Carlo toolkit (Geant4 10.4. 02). Patient Table is made by DICOM image.

2. Materials and Methods

2-1. Validation of the Monte Carlo scheme

We used Geant4 (ver. 10. 4, Geant4 Collaboration)^{11~13)} as a Monte Carlo toolkit and simulated PET device (Discovery ST Elite [GE Medical Systems, Milwaukee, WI, USA]). **Fig. 1** shows the appearance of PET device and scatter phantom^{14~16)}. We compared data from literature and the SF_{fix} obtained from the scatter phantom of NEMA standard to verify the validity of these geometries.

2-2. $SF_{\rm sim}$ and $SF_{\rm hdr}$ in clinical PET/CT examination

We used the data obtained from 15 patients (male: female = 7:8, BMI = $23.0 \pm 3.60 \text{ kg/m}^2$) who underwent a PET/CT scan using Discovery ST Elite at Hirosaki University Hospital between November 2016 and January 2017. The study was approved by the research ethics board of Hirosaki University (2016-047). We subsequently extracted data from patients who did not have any lesions in accordance with the Japanese acquisition guideline $^{6,7)}$. All patients were injected with 200 MBq of 18 F-FDG intravenously, and their images were collected 60 min after injection for 3 min/bed position. PET images were reconstructed by three-dimensional ordered subset expectation

maximization (3D-OSEM) using 20 subsets and 2 iterations. A Gaussian filter of 5.14 mm full width at half maximum (FWHM) was used for spatial smoothing, and the standard filter was also used as a Zaxis filter. We made digital anthropomorphic phantoms from DICOM CT images. We also investigated the percentage of subcutaneous fat as it has an effect on SF to total body area using Weka¹⁷⁾ mounted on ImageJ/Fiji¹⁸⁾. Based on the PET image values, 511 keV gamma rays were emitted. We estimated SF_{sim} in each acquisition bed position. The bed position corresponds to the neck, thorax, and abdomen, except for the brain and bladder. We performed a Monte Carlo simulation until the fractional standard deviation (FSD), which is equal to standard deviation divided by the mean¹⁹⁾, was $\leq 2\%$. In NEMA NU 2-2001²⁰⁾, the range of counts to estimate $SF_{\rm fix}$ is limited to the 120 mm radius from the center of the PET gantry. However, we estimated SFsim under the condition that the range restriction was lifted and expanded to transaxial FOV to simulate an actual PET examination. We also obtained the SF_{hdr} in each acquisition bed position from DICOM header. A Paired t test was used for statistical analysis including the relationship between SF_{sim} and SF_{hdr} . P < 0.05 was considered significant.

2-3. Calculation of NEC and visual assessment

We calculated NECpatient and NECdensity using counts obtained from the evaluation range $^{6,7)}$. NEC_{patient} and NEC_{density} can be calculated using the following formulas:

$$NEC_{i} = (1 - SF)^{\frac{2}{2}} \frac{(P_{i} - R_{i})^{2}}{(P_{i} - R_{i}) + (1 + k)R_{i}} [Mcounts]$$

$$NEC_{patient} = \frac{\sum_{i=1}^{n} - NEC_{i}}{x/100} [Mcounts]$$
(2)

$$NEC_{density} = \frac{\sum_{i=1}^{n} - NEC_{i}}{V_{patient}} \times 1,000 [Mcounts]$$
(3)

$$NEC_{density} = \frac{\sum\limits_{i=1}^{\sum} -NEC_i}{V_{batient}} \times 1,000 [Mcounts]$$
 (3)

Where P_i and R_i represent the prompt and random coincidences of each bed position, respectively. SF represents the scatter fraction. The number of beds that were needed to cover the evaluation range is represented by n. The length of the evaluation range (axial direction) is represented by x (cm). The random scaling factor is represented by k (k = 1): if the random coincidences are measured directly by the delayed coincidence technique, and k = 0: if the random coincidences are estimated from singles). In this study, k = 0 was used. Patient volume within the evaluation range is represented by V_{patient} (cm³).

Visual assessment was performed by four radiologic technologists with at least 5 years of experience in nuclear medicine. They evaluated PET image quality using the five-grade evaluation (Visual score 5: Very good quality, 4: sufficiently good quality, 3: scarcely sufficient quality, 2: not sufficient quality, 1: unreadable) as per the Japanese acquisition guideline^{6,7)}. We conducted a comparative analysis of the NEC values that were obtained using SFsim, and SFhdr to determine whether SF_{fix} were reasonable values. Pearson's correlation coefficient between the BMI and the NECs were calculated and Spearman rank correlation coefficients were calculated for the visual score and the NECs to determine their relationship. Bonferroni's multiple comparison test was used to compare NEC_{patient} and NEC_{density} that were obtained using SF_{fix} , SF_{sim} , and SF_{hdr} . P < 0.05 was considered significant.

3. Results

3-1. Validation of the Monte Carlo scheme

We compared data from literature (SF_{fix} = 0.34^{16}) and the $SF_{\rm fix}$ obtained from the scatter phantom of NEMA standard by using Monte Carlo simulation, to

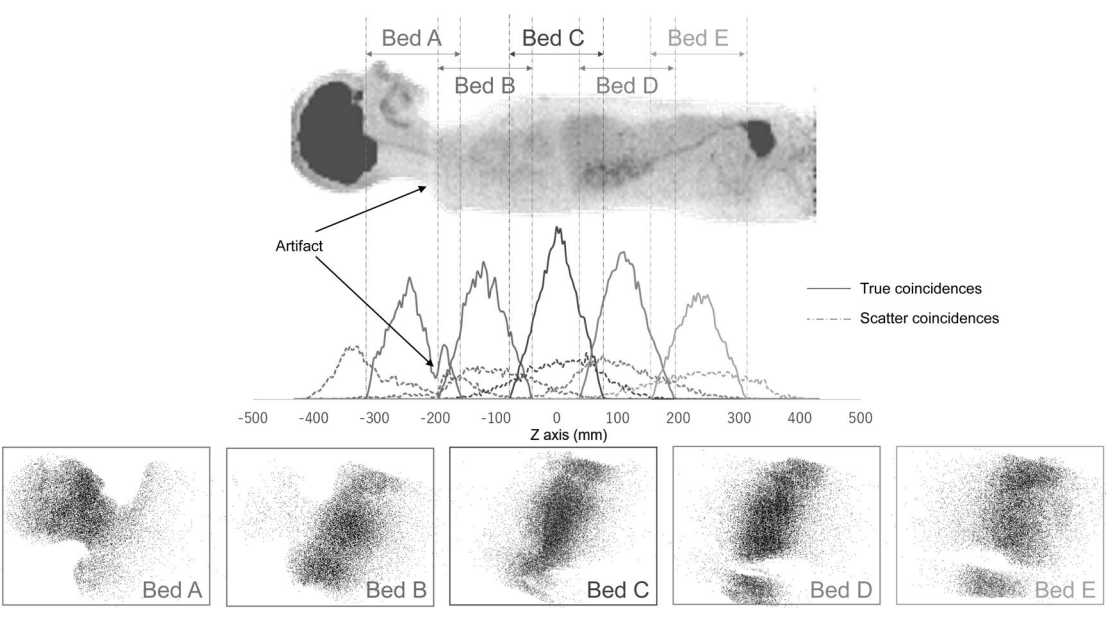


Fig. 2 The original source distribution which were counted as a coincidence count. Many scatter coincidences which are generated from brain region were counted in Bed A position.

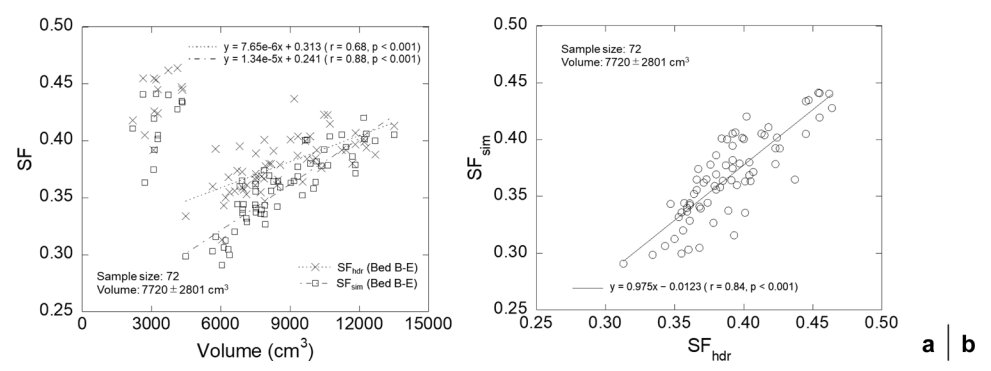


Fig. 3 Fig. 3a shows the relationship between SF_{sim} and SF_{hdr} and patient volume. High SF was obtained from the bed A position in the group where patient volumes were small. SF_{sim} increased lineally with strong correlation (>0.8) in bed B-E position. Fig. 3b shows the relationship between SF_{sim} and SF_{hdr} . SF_{hdr} is slightly higher than SF_{sim} and there. There is a strong correlation between them.

verify the validity of the constructed geometries. The SF_{fix} values estimated was 0.34. From these results, we confirmed that the geometry was constructed properly.

3-2. SF_{sim} and SF_{hdr} in clinical PET/CT examination

Fig. 2 shows the axial profiles of the radioactive source, which were counted from each bed position. The peak of true coincidences was situated at the middle of the bed position, but the peak of the scatter coincidence is not, necessarily. Many scatter coincidences were counted from the brain in bed position A. The relationship between SFs (SF_{sim} and SF_{hdr}) that was obtained from each bed position and patient volume within the range of the bed is given in Fig. 3a. The SF_{sim} and SF_{hdr} distribution was divided into two groups. The SF_{sim} obtained from the bed position A was high, although the patient volume was small. The volume of trunk of the body (Bed B-E) was 4,000-13,500 cm³. The largest percentage of subcutaneous fat was 35% in this study. The discussion was limited only to beds B-E, and the SF_{sim} and SF_{hdr} values were 0.357 ± 0.0316 and 0.379 ± 0.0232 , respectively. The correlation coefficient between SF_{sim} and patient volume was 0.879, and between SF_{hdr} and patient volume was 0.681. In all bed positions, SF_{hdr} was a slightly higher than SF_{sim} with a significant difference (p<0.001) as shown in **Fig. 3b**,

although there was a strong correlation between the SFs (r = 0.836).

3-3. Calculation of the NEC and visual assessment

NEC_{patient} that was obtained using SF_{fix}, SF_{sim}, and SF_{hdr} were 34.2 ± 5.51 , 34.2 ± 7.42 , and 31.5 ± 6.20 , respectively. The results showed that there were significant differences between NECpatient that was obtained using SF_{fix} and SF_{hdr} (p < 0.001) and using SF_{sim} and SF_{hdr} (p < 0.001). NEC_{density} that was obtained using SF_{fix} , SF_{sim} , and SF_{hdr} were 0.639 \pm 0.197, 0.646 ± 0.239 , and 0.594 ± 0.212 , respectively. The results showed that there were significant differences between NEC_{density} that was obtained using SF_{fix} and SF_{hdr} (p < 0.001) and using SF_{sim} and SF_{hdr} (p < 0.001). The relationship between BMI and $\mathrm{NEC}_{\mathrm{patient}}$ and $\mathrm{NEC}_{\mathrm{density}},$ which was obtained using SF_{fix} , SF_{sim} , and SF_{hdr} , respectively, is given in **Fig. 4a**. The correlation coefficients between BMI and NEC_{patient} that was obtained using SF_{fix}, SF_{sim}, and SF_{hdr} were -0.619, -0.757, and -0.771, respectively. The correlation coefficients between BMI and NEC_{density} obtained using SF_{fix}, SF_{sim}, and SF_{hdr} were -0.842, -0.860, and -0.861, respectively. The relationship between visual assessment and NEC_{patient} and NEC_{density} is shown in **Fig. 4b**. Visual score was 3.32 ± 0.814 . The correlation coefficients between the visual assessment and NEC_{patient} that was obtained

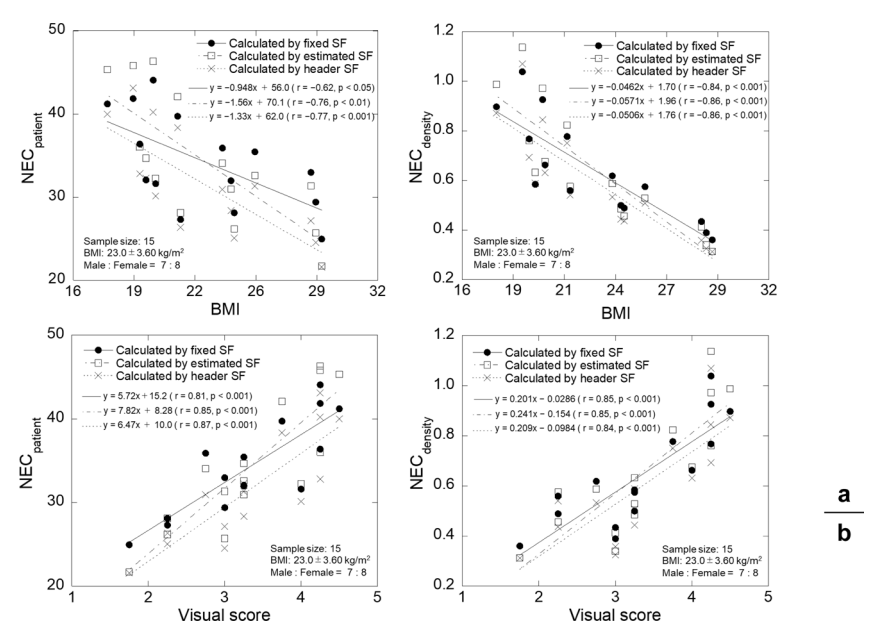


Fig. 4 Fig. 4a shows the correlation between the BMI and the NEC that was obtained using $SF_{\rm fix}$ and $SF_{\rm sim}$. Fig. 4b shows a correlation between the visual assessment and the NEC that was obtained using $SF_{\rm fix}$ and $SF_{\rm sim}$. Visual score representative of an average of 4 evaluators.

using SF_{fix} , SF_{sim} , and SF_{hdr} were 0.813, 0.845, and 0.869, respectively. The correlation coefficients between visual assessment and $NEC_{density}$ that was obtained using SF_{fix} , SF_{sim} , and SF_{hdr} were 0.845, 0.847, and 0.841, respectively.

4. Discussion

4-1. $SF_{\rm sim}$ and $SF_{\rm hdr}$ in clinical PET/CT examination

High SF_{sim} and SF_{hdr} were obtained from the bed position A in the group where patient volumes were small. Bed A is equivalent to the range of the face or neck. Multiple scattered radiations were counted from the brain at the bed position A as shown in **Fig. 2**. The use of a shield may be considered²¹⁾ depending on the situation, such as evaluation of carotid plaque. Previous studies^{22,23)} reported that the use of a shield was not effective in brain PET examinations. However, in this case, the number of radioisotopes existing out-of-axial FOV is much greater, unlike that for brain PET. We estimated the SF_{sim} of the cylindrical phantom with diameters of

10-50 cm in a previous study²⁴. The SF_{sim} increased by 1.3 times while changing the diameter of cylindrical phantom with line source from 20 cm to 30 cm. In this study, the volume of the trunk of the body (Bed B-E) was 4,000-13,500 cm³. Because axial FOV is 15.7 cm, these are corresponding to the volume of cylinder with a diameter of 19-33 cm. SF_{sim} increased from 0.44 to 0.57 (1.3 times) in this study. Therefore, SF_{sim} increment was the same. We also concluded SFsim is influenced by FDG distribution inside of the patient's body as seen in previous study. The calculated SF_{sim} increased from 44% to 47.5% (1.08 times) when the source distribution ratio in a cylindrical phantom with a 20 cm diameter was changed from 100% (uniform distribution) to 64%²⁴. Judging from the ratio of subcutaneous fat in the CT image, the bias of FDG distribution was not large (from 100% to 65%) in this study. The difference of the FDG distribution inside of the patient's body was reflected in this result and such level variation was by the effect of the FDG distribution, but also by

statistical error in the Monte Carlo calculation. SF_{hdr} is not used for NEC calculation in Japanese acquisition guideline because calculation method is unclear. **Fig. 3b** shows the accuracy and tendency. SF_{hdr} are reflecting the difference of the patient size. However, there was significant difference between SF_{sim} and SF_{hdr} . SF_{hdr} written in DICOM tag (0054, 1323) means an estimate of the fraction of acquired counts that were due to scatter and were corrected in image. Thus, if we assume SF_{sim} is a true value, scatter correction could not accurately correct by removing the accurate quantity of scattered radiation when there is large difference between SF_{sim} and SF_{hdr} . The accuracy depends on the kind of PET device used; thus, further study is required, either way.

4-2. Calculation of the NEC and visual assessment

We calculated NEC_{patient} and NEC_{density} from the data of 15 patients. Similarly, in a previous study 10 , a strong correlation was found between NEC_{patient} and visual assessment, and NEC_{density} and visual assessment (> 0.8). This result was obtained from a single facility, and relative evaluation was performed between images obtained from there. The same correction and reconstruction algorithm were used, and the impact of scattered radiation from out-of-axial FOV was mostly the same.

The results showed that there was no significant difference between the NECs that were obtained using SF_{fix} and SF_{sim}. The correlation coefficient between the BMI and the NEC_{patient}, visual assessment and the NEC_{patient} that was obtained using SF_{sim} and SF_{hdr} increased slightly, but there was no difference significant between the BMI and the NEC_{density}, visual assessment and the NEC_{density} as shown in Fig. 4. It means that to subjective evaluation of a person is difficult and the variation of the visual assessment was larger than the effect of using SF_{sim} for the calculation of NEC. Moreover, the SF_{sim} obtained by Discovery ST Elite took a value within the range of 0.3-0.4. This is the greatest difference, but such difference does not occur in all beds. Including other beds diminishes the effect of the difference of SF_{sim} . From the above results, the use of estimated $SF_{\rm sim}$ for NEC calculation using Discovery ST Elite is not necessary. We can use $SF_{\rm fix}$ in a manner similar to how it was previously used. However, this study did not include extreme obesity patient (such as BMI > 30), as it is unclear whether the $SF_{\rm fix}$ is an appropriate value to use in all cases. Based on the regression line, the NEC_{patient} obtained using $SF_{\rm fix}$ will reach the lower limit (NEC_{patient} > 13) of the Japanese acquisition guideline when BMI is 45.4, NEC_{patient} obtained using $SF_{\rm sim}$ will reach it when the BMI is 36.6. The use of $SF_{\rm sim}$ might be considered for NEC calculations for heavy patients.

5. Conclusion

We uncovered the relationship among $SF_{\rm fix}$, $SF_{\rm sim}$, and $SF_{\rm hdr}$. There was no significant difference between the NEC obtained using $SF_{\rm fix}$ and $SF_{\rm sim}$ based on standard proportion. However, there were significant differences between the NEC obtained using $SF_{\rm sim}$ and $SF_{\rm hdr}$. The results of the PET device used in this study showed that $SF_{\rm fix}$ could be used as a representative value. Moreover, using $SF_{\rm fix}$ is more appropriate than $SF_{\rm hdr}$ in NEC calculations.

References

- Skougaard K, Nielsen D, Jensen BV, et al: Comparison of EORTC criteria and PERCIST for PET/CT response evaluation of patients with metastatic colorectal cancer treated with irinotecan and cetuximab. J Nucl Med, 54(7): 1026–1031, 2013
- Kim HD, Kim BJ, Kim HS, et al: Comparison of the morphologic criteria (RECIST) and metabolic criteria (EORTC and PERCIST) in tumor response assessments: a pooled analysis. Korean J Intern Med, 34 (3): 608-617, 2019
- Adams MC, Turkington TG, Wilson JM, et al: A systematic review of the factors affecting accuracy of SUV measurements. AJR Am J Roentgenol, 195(2): 310–320, 2010
- 4) Westerterp M, Pruim J, Oyen W, et al: Quantification of FDG PET studies using standardised uptake values in multi-centre trials: effects of image reconstruction, resolution and ROI definition parameters. Eur J Nucl Med Mol Imaging, 34(3): 392-404, 2007

- Reynés-Llompart G, Sabaté-Llobera A, Llinares-Tello E, et al: Image quality evaluation in a modern PET system: impact of new reconstructions methods and a radiomics approach. Sci Rep, 9(1), doi: 10.1038/ s41598-019-46937-8, 2019
- 6) Fukukita H, Senda M, Terauchi T, et al: Japanese guideline for the oncology FDG-PET/CT data acquisition protocol: synopsis of Version 1.0. Ann Nucl Med, **24**(4), 325–334, 2010
- Fukukita H, Suzuki K, Matsumoto K, et al: Japanese guideline for the oncology FDG-PET/CT data acquisition protocol: synopsis of Version 2.0. Ann Nucl Med, 28(7): 693–705, 2014
- Wickham F, Mcmeekin H, Burniston M, et al: Patientspecific optimisation of administered activity and acquisition times for ¹⁸F-FDG PET imaging. EJNMMI Res, https://doi.org/10.1186/s13550-016-0250-3, 2017
- 9) 島田直毅, 大崎洋充, 村野剛志, 他:FDG-PET/ CT 検査における物理学的指標に基づいた収集時 間の最適化. 日本放射線技術学会雑誌, **67**(10): 1259-1266, 2011
- 10) Mizuta T, Senda M, Okamura T, et al: NEC density and liver ROI S/N ratio for image quality control of whole-body FDG-PET scans: comparison with visual assessment. Mol Imaging Biol, 11(6): 480-486, 2009
- Agostinelli S, Allison J, Amako K, et al: Geant4—a simulation toolkit. Nucl Instrum Methods A, 506: 250–303, 2006
- Allison J, Amako K, Apostolakis J, et al: Geant4 developments and applications. IEEE Trans Nucl Sci, 53: 270-278, 2006
- 13) Allison J, Amako K, Apostolakis J, et al: Recent developments in Geant4. Nucl Instrum Methods Phys Res Sect A, 835: 186-225, 2016
- 14) Mawlawi O, Podoloff DA, Kohlmyer S, et al: Performance characteristics of a newly developed PET/CT scanner using NEMA standards in 2D and 3D modes. J Nucl Med, 45(10): 1734-1742, 2004
- Macdonald LR, Schmitz RE, Alessio AM, et al: Measured count-rate performance of the Discovery

- STE PET/CT scanner in 2D, 3D and partial collimation acquisition modes. Phys Med Biol, **53** (14): 3723–3738, 2008
- 16) Macdonald LR, Schmitz RE, Alessio AM, et al: Count-Rate Performance of the Discovery STE PET Scanner Using Partial Collimation. IEEE Nucl Sci Symp Conf Rec, 4: 2488-2493, 2006
- 17) Arganda-Carreras I, Kaynig V, Rueden C, et al: Trainable Weka Segmentation: a machine learning tool for microscopy pixel classification. Bioinformatics, 33(15): 2424–2426, 2017
- Schindelin J, Arganda-Carreras I, Frise E, et al: Fiji: an open-source platform for biological-image analysis. Nat Methods, 9(7): 676-682, 2012
- 19) Dupree SA, Fraley SK: A Monte Carlo Primer: A Practical Approach to Radiation Transport: 35–38, Springer-Verlag, New York, 2002
- 20) National Electrical Manufacturers Association: NEMA Standards Publication NU 2-2001: Performance Measurement of Positron Emission Tomographs. Rosslyn, VA: National Electrical Manufacturers Association, 2001
- 21) Hasegawa T, Murayama H, Matsuura H, et al: Shielding effects of body – shields for 3D PET. Jpn J Med Phys, 22(4): 318–326, 2002
- 19) Konik A, Madsen MT, Sunderland JJ: GATE simulations of human and small animal PET for determination of scatter fraction as a function of object size. IEEE Trans Nucl Sci, 59(5): 2558–2563, 2010
- 22) Ibaraki M, Sugawara S, Nakamura K, et al: The effect of activity outside the field-of-view on image signal-tonoise ratio for 3D PET with ¹⁵O. Physics in medicine and biology, 56(10), 3061-3072, 2011
- 23) Wagatsuma K, Oda K, Miwa K, et al: Effects of a novel tungsten-impregnated rubber neck shield on the quality of cerebral images acquired using ¹⁵O-labeled gas. Radiol Phys Technol, 10(4), 422–430, 2017
- 24) Hosokawa S, Inoue K, Kano D, et al.: A simulation study for estimating scatter fraction in whole-body (18) F-FDG PET/CT. Radiol Phys Technol, 10 (2): 204-212, 2017